NAVSWC TR 91-182

AD-A241 957

(1)

EFFECTIVE DYNAMIC MATERIAL PARAMETERS AND LOCALIZED SCATTERING

BY KURT P. SCHARNHORST

RESEARCH AND TECHNOLOGY DEPARTMENT

20 MARCH 1991

Approved for public release; distribution is unlimited.

NAVAL SURFACE WARFARE CENTER

Dahlgren, Virginia 22448-5000 • Silver Spring, Maryland 20903-5000

EFFECTIVE DYNAMIC MATERIAL PARAMETERS AND LOCALIZED SCATTERING

BY KURT P. SCHARNHORST
RESEARCH AND TECHNOLOGY DEPARTMENT

20 MARCH 1991

NAVAL SURFACE WARFARE CENTER
Dahlgren, Virginia 22448-5000 • Silver Spring, Maryland 20903-5000

FOREWORD

This report is based on theoretical studies presented in Naval Surface Warfare Center (NAVSWC) Acoustics Group Letter Reports LR-109 entitled "Effective Dynamic Material Parameters of Inhomogeneous Materials. I. Preliminary Results Based on the T-Matrix for a Pair of Spherical Scatterers," of 21 March 1989 and LR-117 entitled "Effective Dynamic Material Parameters of Inhomogeneous Materials. II. Multiple Scattering and Mode Conversion," of 10 September 1990.

Effects of localized multiple scattering on the longitudinal wave vector of coherent waves in inhomogeneous materials are studied. A new wave vector is derived by replacing the single particle far field forward scattering amplitude by the average pair scattering amplitude. The Perkus-Yevick hard sphere radial distribution function is used to average over the separations of scatterers. The results are applied to mass loaded polyurethane spheres in syntactic foam, a type of material potentially significant in Naval applications and to lead spheres in epoxy resin. In the case of lead in epoxy, it is found that the pair scattering mechanism significantly alters the real and imaginary parts of the effective wave vector and the mode conversion scattering cross section. Only negligible effects are observed in mass loaded polyurethane in syntactic foam.

This work was sponsored by the NAVSWC IR Program and the Mines Block Program/Mine Supporting Technology/Covert Materials (Code U077).

The author wishes to thank Mrs. Linda Tsui (E52) for transferring our 'Pair Scattering Algorithm' to the Naval Research Laboratory Supercomputer and running it to obtain the data documented in this report.

Approved by:

Carl E. Mueller

CARL E. MUELLER, Head
Materials Division

CONTENTS

ILLUSTRATIONS

ILLUSTRATIONS (Cont.)

TABLES

INTRODUCTION

The present paper is based on NAVSWC Acoustics Group Letter Reports LR-109 entitled "Effective Dynamic Material Parameters of Inhomogeneous Materials. I. Preliminary Results based on the T-Matrix for a Pair of Spherical Scatterers" dated 3/21/89 and LR-117 entitled "Effective Dynamic Material Parameters of Inhomogeneous Materials. II. Multiple Scattering and Mode Conversion" dated 9/10/90. The essential elements of this work were also reported at professional society meetings.[1]

As stated in LR-109, the purpose of the work was to explore the possibility of including in the classical theory for the effective wave vector certain localized multiple scattering events which have thus far been ignored. Replacing the single particle longitudinal far field forward scattering amplitude, $f_p(1,0)$, by the corresponding (averaged) pair scattering amplitude, $f_p(2,0)$, achieves this objective. Effects of mutual dynamic loading of scatterers, as well as multiple scattering between nearest neighbors will be accounted for and, if important, will show up in the effective parameters, particularly as the concentration of scatterers is increased. It should however be realized that the classical theory strictly applies only to low concentrations of inclusions and/or weak scattering. In the present work, we are mainly interested in high concentrations and strong scattering such that the product of the number density of inclusions, n, times the extinction cross section, σ_e, is much larger than unity near resonance. This means that power loss per unit length due to scattering and absorption is much greater than 1/e, the coherent wave is strongly attenuated and the classical theory not strictly applicable. The present results must therefore be compared with experiment to test their validity. This cannot be emphasized strongly enough. Using the far field scattering amplitude in a dense medium and neglecting possible near field effects, as is done here, although conceptually attractive, can at best only be a heuristic approach to the problem.

In LR-109 we presented an analysis of the algorithm for the T-Matrix of a pair of scatterers, the latter being the essential ingredient in this type of calculation. Preliminary estimates of the effective attenuation and wave speeds of longitudinal waves in inhomogeneous syntactic foam with silicone inclusions and in rubber with air bubbles were also presented. The calculations were preliminary in the sense that only the spatial orientation average of a pair of scatterers was accounted for in $f_p(2,0)$ and constant nearest neighbor distances were assumed for given volume concentrations, the latter being representative of a regular lattice rather than a random medium. There was also a problem with the convergence of the algorithm whenever the maximum mode number exceeded certain low values. Only very restricted ka-ranges could be explored.

The convergence problem (due to the large integer storage limitation of the NAVSWC CDC 860 computer (see also LR-117)) was solved subsequently and the algorithm applied to two different inhomogeneous systems; mass loaded polyurethane in syntactic foam and lead in epoxy resin (NAVSWC Acoustics Group Letter Report LR-117). The new ingredient in the latter work was the use of the Perkus-Yevick pair distribution function for the statistical distribution of nearest neighbor separations in a random distribution of spherical inclusions in an inhomogeneous solid.

The body of the present paper is essentially a reprint of NAVSWC Acoustics Group Letter Report LR-117. The Appendix was taken from NAVSWC Acoustics Group Letter Report LR-109. The other data presented in LR-109, although correct, is incomplete because of the convergence problem cited above and has therefore not been included in the present summary.

THE MODIFIED CLASSICAL EXPRESSION FOR THE EFFECTIVE WAVE VECTOR

The classical expression for the effective wave vector of longitudinal waves in inhomogeneous media is:[2]

$$k_p^* = k_p + 2\pi n f_p(1,0)/k_p \qquad (1)$$

where $k_p = \omega/c_p$, c_p is the longitudinal wave speed of the matrix material and $f_p(1,0)$ the far field longitudinal forward scattering amplitude of a single scatterer. Replacing n by the volume concentration of spherical scatterers of radius a, $\phi = 4\pi na^3/3$, we have:

$$k_p^* = k_p[1 + (3\phi/k_p^2a^3)f_p(1,0)/2] \qquad (2)$$

Equations 1 and 2 show that $\Delta k_p \equiv (k_p^* - k_p)$ is proportional to n times the far field scattering contribution of a single scatterer scattering independently. We wish to replace this term by a quantity proportional to $\bar{f}_p(2,0,\phi)$, the volume concentration dependent average of the far field forward scattering amplitude of a pair of scatterers, where the average has to be performed with respect to all orientations and over a range of separations of scatterers. In so doing, the modified version of the equation will account for the mutual dynamic loading of scatterers in close proximity and for all orders of mutual scattering events between pairs.

The orientation average of $f_p(2,0)$, the far field forward scattering amplitude of an isolated pair of scatterers, may be performed analytically. The result is given below. For the radial average we use the volume concentration dependent Percus-Yevick hard sphere radial distribution function, $g(\phi,r)$.[3] Accordingly, the average number of scatterers with centers within dr at the radial distance r from any other scatterer is

$$N(\phi,r) = 4\pi n g(\phi,r) r^2 dr$$

Since we only wish to consider unobstructed pairs of scatterers in $f_p(2,0)$, those not having intervening neighbors, we have to choose a cutoff radius for $g(\phi,r)$. In the present work we have explored the first nearest neighbor maximum of $g(\phi,r)$, R_0, as a cutoff. Defining the probability of finding the center of another scatterer within dr at the radial distance r from any other scatterer as

$$P(\phi,r)dr = \frac{\text{The number of centers in the shell between } r \text{ and } r + dr}{\text{The number of centers in the shell between } 2a \text{ and } R_0}$$

we have

$$P(\phi,r)dr = \frac{g(\phi,r)r^2dr}{\int_{2a}^{R_0} g(\phi,r)r^2dr} = \frac{g(\phi,x)x^2dx}{\int_1^{x_0} g(\phi,x)x^2dx} = p(\phi,x)dx \tag{3}$$

where $x = r/2a$ and $x_0 = R_0/2a$. The average pair scattering amplitude per scatterer at the volume concentration ϕ is therefore

$$\bar{f}_p(2,0,\phi) = \int_1^{x_0} p(\phi,x)\, f_p(2,0,x)\,dx \tag{4}$$

where $f_p(2,0,x)$ is the average of $f_p(2,0)$ over all directions of the incident wave with respect to the axis of the pair. The average pair scattering amplitude per unit volume at the volume concentration ϕ is therefore

$$F_p(2,0,\phi) = (n/2)\bar{f}_p(2,0,\phi) \tag{5}$$

where the factor 1/2 accounts for the fact that on making the change from the average pair scattering amplitude per scatterer to that per unit volume, all pairs are counted twice.

Replacing the quantity $nf_p(1,0)$ in Equation (1) by $F_p(2,0,\phi)$ we obtain the modified classical wave vector

$$\vec{k}_p = k_p + \pi n\bar{f}_p(2,0,\phi)/k_p \tag{6}$$

or

$$\bar{k}_p^* = k_p + (3\phi/4k_pa^3)\frac{\int_1^{x_0} f_p(2,0,x)\, g(\phi,x)x^2dx}{\int_1^{x_0} g(\phi,x)x^2dx} \tag{7}$$

which shows explicitly that the linear dependence of the effective wave vector on ϕ in Equation (2) has now become nonlinear in terms of $g(\phi,x)$. From Equations (2) and (7), we obtain expressions for the reduced wave speed and the attenuation coefficient at given volume concentrations. In general, if k is the wave vector of the matrix and $\bar{k}$ that of the composite, we have

$$\bar{k} = (\omega/\bar{c}) + i\bar{\alpha}$$

$$(\bar{c}/c) = k/\mathrm{Real}(\bar{k}) \tag{8}$$

and

$$\text{Attenuation/unit length} = 8.69\,\mathrm{Im}(\bar{k}) = -10\log_{10}[e^{-2\mathrm{Im}(\bar{k})}] \tag{9}$$

where, in Equation (8), we have assumed that the matrix medium is elastic. Plots of Equations (8) and (9) are given below for single particle and pair scattering at different volume concentrations of inclusions.

LONGITUDINAL FAR FIELD FORWARD SCATTERING AMPLITUDES AND SCATTERING CROSS SECTIONS

The longitudinal forward scattering amplitude of isolated spherical scatterers in terms of the T-Matrix is.[4,5]

$$f_p(1,0) = (1/ik_p)\sum_{n=0}^{\infty}(2n+1)T_n^{11} \tag{10}$$

where T_n^{11} is the element T_{nn}^{11} of T^{11}, a diagonal matrix (see the Appendix for more details). In addition to the attenuation (extinction) coefficient and the wave speed which follow from Equations (1), (8), (9), and (10), it is also of interest to study the absorption coefficient and the scattering cross sections. There are three types of scattering cross sections which are of interest here, σ_{pp}, the longitudinal to longitudinal wave scattering cross section, σ_{ps}, the longitudinal to shear wave (mode conversion) cross section and σ_a, the absorption cross section. For isolated spherical scatterers the first two of these are[4,5]

$$\sigma_{pp}(1) = (4\pi/k_p^2)\sum_{n=0}^{\infty}(2n+1)\left|T_n^{11}\right|^2 \tag{11}$$

$$\sigma_{ps}(1) = (4\pi/k_p^2)\sum_{n=0}^{\infty}(2n+1)\left|T_n^{31}\right|^2 \tag{12}$$

The absorption cross section is non-zero only if the inclusion material is viscoelastic. We assume the matrix material to be elastic. The absorption cross section may be obtained by means of the Forward Scattering Theorem, according to which the forward scattering amplitude, $f_p(\hat{k}_p,\hat{k}_p)$ is related to the cross sections as[4,6,7]

$$(4\pi/k_p)\mathrm{Im}[f_p(\hat{k}_p,\hat{k}_p)] = \sigma_{pp} + \sigma_{ps} + \sigma_a = \sigma_e \tag{13}$$

where σ_e is the extinction (attenuation) cross section. Equation (13) is perfectly general result, applying to any matrix/scatterer combination and scatterer shape, including any cluster of scatterers, such as a pair and regardless of whether the scatter is elastic or viscoelastic. In fact it applies to any kind of scattering phenomenon and is used extensively in such diverse fields as astronomy, nuclear and elementary particle scattering, radar propagation, medical diagnostics, etc. Using Equations (10), (11), and (12) in Equation (13) we obtain $\sigma_a(1)$ for single scatterers.

The absorption coefficient follows from the definition

$$\text{Absorption/unit length} = -10\log_{10}[e^{-n\sigma_a(1)}] = 4.343n\sigma_a(1) \tag{14}$$

With the aid of Equations (1), (9), and (13) this may be written

$$\text{Absorption/unit length} = \text{Attenuation/unit length} - 4.343n[\sigma_{pp}(1) + \sigma_{ps}(1)] \qquad (15)$$

for single scatterers. For pairs of scatterers we simply replace n by n/2 and the single particle scattering cross sections $\sigma_{pp}(1)$, $\sigma_{ps}(1)$, $\sigma_a(1)$ by the corresponding pair scattering cross sections $\sigma_{pp}(2)$, $\sigma_{ps}(2)$ and $\sigma_a(2)$.

Since Equation (13) holds for any orientation and any separation of a pair of scatterers it also holds for the averaged quantities

$$(4\pi/k_p)\mathrm{Im}[\bar{f}_p(2,0,\phi)] = \bar{\sigma}_{pp} + \bar{\sigma}_{ps} + \bar{\sigma}_a \qquad (16)$$

where the bars denote orientation plus separation averages. Hence the average absorption cross section for a pair follows from Equation (16) and the average absorption coefficient from Equation (14) with n replaced by n/2 and $\sigma_a(1)$ replaced by $\bar{\sigma}_a$. In our plots of cross sections we have normalized those for single particles by πa^2 and those for two particle averages by $2\pi a^2$. The latter does not represent the true average of the geometrical cross section of a pair but the definition is convenient since the two cross sections should (and do) approach each other at very large particle separations.

As mentioned above, the Perkus-Yevick average over radial separations must be done numerically, while that over angular orientations of the axis of the pair with respect to the incident plain wave direction may be done analytically. The result of the orientation average, assuming a uniform angular distribution, in terms of the T-Matrix elements of a pair of scatterers is

$$f_p(2,0,x) = (l/ik_p) \lim_{l_{max}\to\infty} \left(\sum_{m=0}^{l_{max}} \sum_{l=0}^{l_{max}-m} \varepsilon_m T^{ee(11)}_{m\,l,l} \right) \qquad (17)$$

$$\sigma_{pp} = (4\pi/k_p^2) \lim_{l_{max}\to\infty} \left(\sum_{m=0}^{l_{max}} \sum_{l,l'=0}^{l_{max}-m} \varepsilon_m \left| T^{ee(11)}_{m\,l,l'} \right|^2 \right) \qquad (18)$$

$$\sigma_{ps} = (4\pi/k_p^2) \lim_{l_{max}\to\infty} \left(\sum_{m=0}^{l_{max}} \sum_{l,l'=0}^{l_{max}-m} \varepsilon_m \left\{ \left| T^{oe(41)}_{m\,l,l'} \right|^2 + \left| T^{ee(51)}_{m\,l,l'} \right|^2 \right\} \right) \qquad (19)$$

where $\varepsilon_m = 2-\delta_{m,o}$. The analysis of the T-Matrix of a pair of scatterers in terms of the T-Matrices of the individual scatterers is given in Reference 8. Substituting Equation (17) into Equations (4) and (7) yields $\bar{f}_p(2,0,\phi)$ and $\bar{k}_p{}^*$, respectively. Averaging σ_{pp} and σ_{ps} in Equations (18) and (19) with respect to $p(\phi,x)$ from $x=1$ to $x=x_0$ yields the averaged cross sections $\bar{\sigma}_{pp}$ and $\bar{\sigma}_{ps}$ in Equation (16).

The super and subscripts on the matrix elements are interpreted as follows: In the Appendix we show that the T-Matrix has the form

$$T = \begin{bmatrix} x_{11} & 0 & 0 & x_{14} & x_{15} & 0 \\ 0 & x_{22} & x_{23} & 0 & 0 & x_{26} \\ 0 & x_{32} & x_{33} & 0 & 0 & x_{36} \\ x_{41} & 0 & 0 & x_{44} & x_{45} & 0 \\ x_{51} & 0 & 0 & x_{54} & x_{55} & 0 \\ 0 & x_{62} & x_{63} & 0 & 0 & x_{66} \end{bmatrix} \tag{20}$$

where the x_{ij} are 'm-diagonal' matrices (Equation (4) of the Appendix). The 2x2 block in the upper left hand corner corresponds to longitudinal scattering, the 4x4 block in the lower right hand corner to shear wave scattering, all others to mode conversion scattering. In particular

$$x_{11} = T^{ee(11)}$$

$$x_{41} = T^{oe(41)}$$

$$x_{51} = T^{ee(51)}$$

The added superscripts on the T-Matrix refer to the parity of the corresponding wave functions, e.g., $T^{oe(41)}$ transforms an even parity longitudinal wave function into an odd parity shear wave function. The first sum in Equations (17), (18), and (19) is the sum over the azimuthal index or the 'm-blocks'. Subsequent sums are over the elements in the 'm-blocks' or the mode numbers. l_{max} is the largest mode number included in the calculations. In the present work $l_{max} = 9$, where $l=0$ corresponds to the monopole, $l=1$ to the dipole, $l=2$ to the quadrupole, etc.

In the case of elastic materials, the T-Matrix must satisfy the equation (T-Matrix Theorem)[4]

$$0 = \mathrm{Real}(T) + T^{t}T^{*} \tag{21}$$

where the superscripts t and * denote the transpose and the complex conjugate respectively. Since T is symmetric in the case of elastic materials this equation may also be written

$$0 = \mathrm{Real}(T) + T\,T^{*}$$

Doing the multiplication indicated in Equation (21) shows that the diagonal elements of -Real [$T^{ee(11)}$], the elements in Equation (17), are, in fact, equal to the combined sums over l' of the elements in Equations (18) and (19), for fixed m and l. This illustrates the fact that the Forward Scattering Theorem for elastic scatterers is a corrolary of the T-Matrix Theorem. In the case of single spherical scatterers, the situation is somewhat simpler algebraically, as may be seen from Equations (12) and (13) in the Appendix.

In the case of viscoelastic inclusions Equations (17), (18), and (19) are still true, but $T^{t} \neq T$ and the left hand side of Equation (21) is not equal to zero. As a consequence, the absorption cross sections in Equations (13) and (16) are not equal to zero.

Since Equations (10), (11), (12), (17), (18), and (19) are true regardless of whether the inclusions are elastic or viscoelastics, the same algorithm was used in both cases to calculate the various cross sections, the attenuation coefficient, the wave speed, and the absorption coefficient in the case of viscoelastic scatterers. In the case of elastic inclusions in elastic matrix materials, we have checked the convergence of our pair scattering algorithm by plotting Equation (9), using the right and left hand sides of Equation (16), as defined by Equations (17), (18), and (19), with $\bar{\sigma}_a$ set to zero. The two curves should be (and are) identical. This shows that in the case of lead in epoxy, choosing $l_{max} = 9$ is sufficient for the calculation of the T-matrix (strictly only for its real part) in the range from $k_pa = .1$ to 1. Figure 1 shows the error. Comparing with the corresponding attenuation curves shows that the error is of order 10^{-4} at worst (at K1*A = 1. ($\equiv k_pa$) for $\phi = 5.2\%$). In the case of viscoelastic inclusions, the difference, as calculated for a viscoelastic polymer in syntactic foam, is due to absorption.

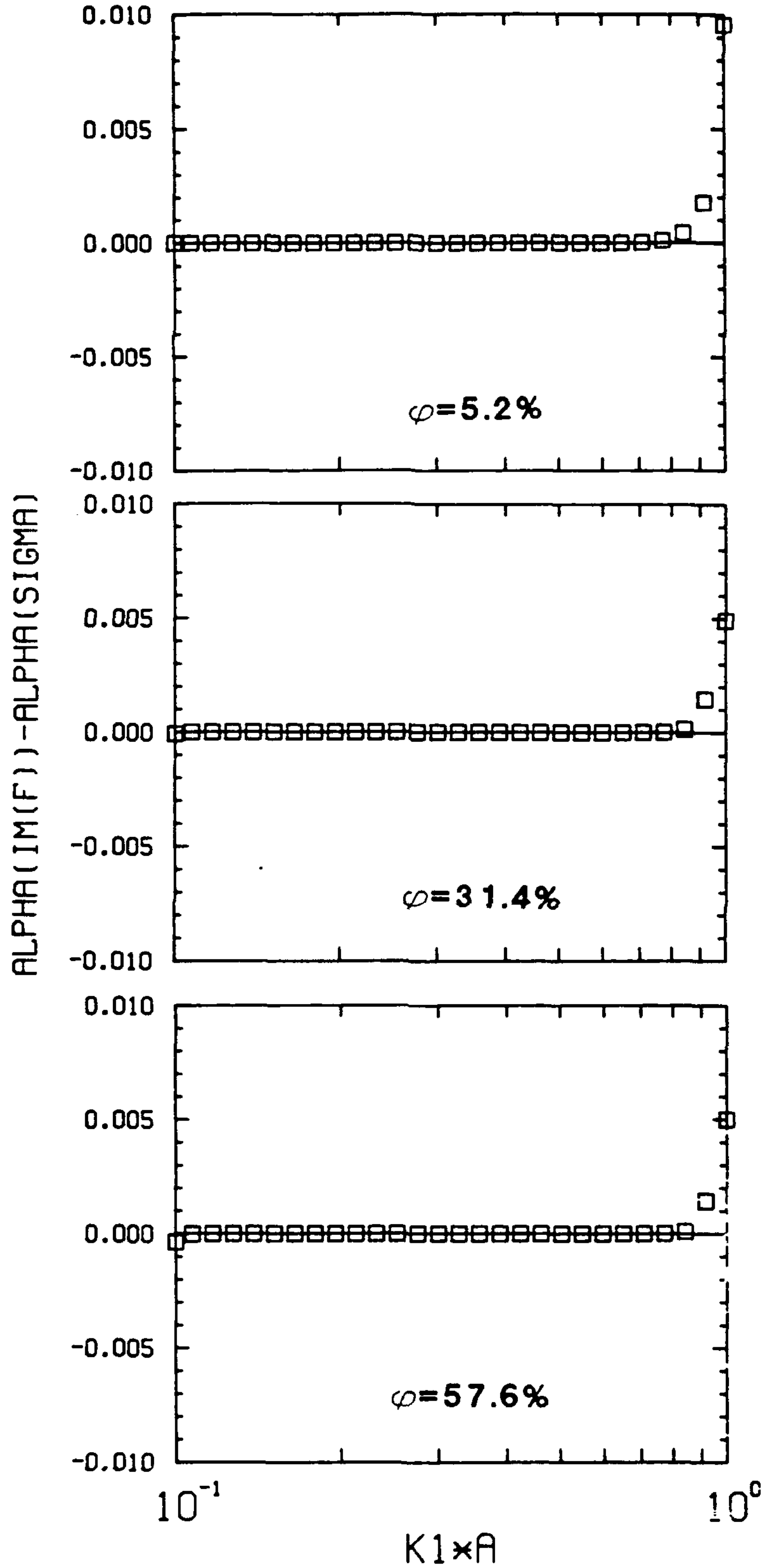

FIGURE 1. THE DIFFERENCE BETWEEN THE ATTENUATION COEFFICIENTS (IN dB/m) DERIVED FROM THE RIGHT AND LEFT HAND SIDES OF THE T-MATRIX EQUATION FOR LEAD IN EPOXY (EPON 828Z)

RESULTS AND DISCUSSION

PRELIMINARIES

To begin with, in Figure 2 we have plotted the three Perkus-Yevick distributions used in the present work.[3] Note the relatively large oscillations at high concentrations of inclusions and the large number of scatterers in contact at 57.6 percent compared to the number at 5.2 percent. These differences determine the nonlinear dependence of k_p on ϕ.

All calculations are for scatterer radii, a($\equiv$ A) of 2 mm. All plots, except those of the radial distribution function, are versus K1*A, where K1 ($\equiv k_p$) is the wave vector of the respective matrix material. The effective wave speeds of inhomogeneous media, <C1>, have been reduced by those of the corresponding matrix media, C1 ($\equiv c_p$).

The material parameters of the components of the two inhomogeneous materials discussed in this work are listed in Table 1. All parameters are assumed to be constant. The polyurethane based elastomer should be thought of as being mass loaded with metal dust in order to achieve the mass density given. It should also be thought of as containing about 10 percent by volume of microscopically dispersed air for enhanced absorption. The order of magnitude of the shear loss tangent of the polyurethane inclusions is typical of the shear loss tangent peak in the relaxation region of this type of modified elastomer.

TABLE 1. MATERIAL PARAMETERS

	ρ(gm/cm^3)	λ*	G_0*	δ*
Syntactic Foam	0.64	0.938	0.344	0.0
Polyurethane	2.64	0.320	0.015	0.45
Epoxy (Epon 828Z)	1.20	2.185	0.769	0.0
Lead	11.3	17.10	3.714	0.0

*Moduli are reduced by 2.25E10 dyne/cm^2
$G = G_0(1\text{-}i\delta)$ = Shear Modulus
λ = First Lamé Parameter

The frequency corresponding to K1*A = .1 in the syntactic foam matrix (sound speed = 2391 m/sec) is 19 kHz (7.6 kHz for A = .5 cm), that in the epoxy matrix (sound speed = 2640 m/sec) is 21 kHz (8.40 kHz for A = .5 cm).

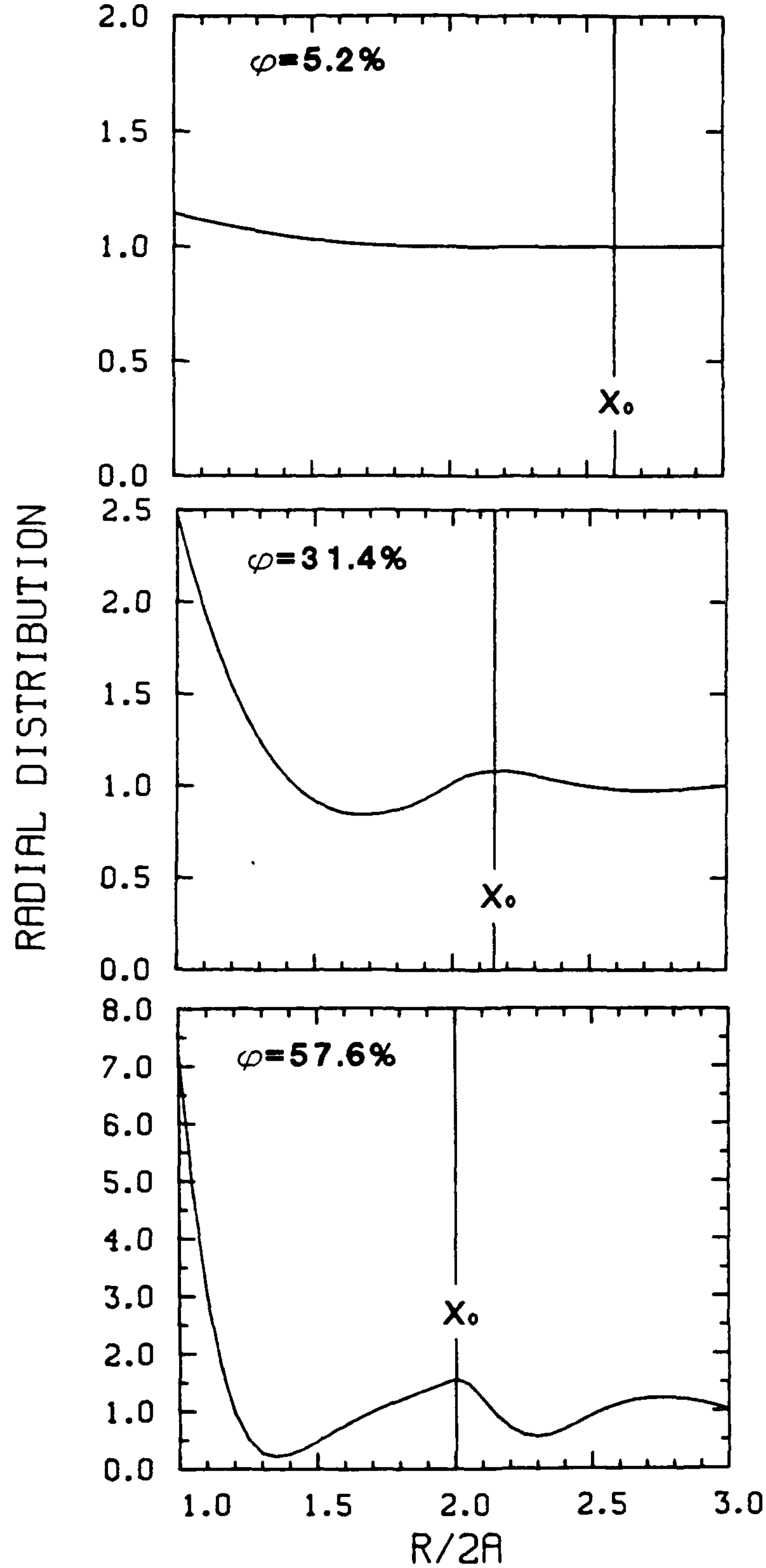

FIGURE 2. THE "HARD SPHERE," PERKUS-YEVICK RADIAL DISTRIBUTION FUNCTION, $g(\phi,x)$.[3] $X_0(\phi) = R_0(\phi)/2A$ IS THE "CUTOFF" RADIUS USED IN THE PRESENT CALCULATIONS

CROSS SECTIONS

The salient features of the frequency dependence of the effective wave speed, attenuation and absorption may be understood best by first considering the various cross sections.

Figures 3 and 4 show that as the volume concentration increases, the pair scattering cross sections broaden in the low frequency, dipole (mode conversion) region and the dipole maxima decrease. The effect is most conspicuous in the case of Pb in epoxy, Figure 3, but appears to saturate above 31.4 percent. Similar remarks apply to urethane in syntactic foam, where the low frequency maximum is due to the dipole, the high frequency maximum to the monopole and intermediate maximum is due to the quadrupole, Figure 4. The absorption cross section is a significant part of the total in the latter case, Figure 4 and the difference between $\sigma_{pp} + \sigma_{ps}$ and σ_{pp} shows that mode conversion is significant in both the dipole and the quadrupole regions of scattering. In the case of 5.2 percent Pb in epoxy, the dipole maximum is clearly shifted to slightly higher frequencies. At higher concentrations the shift is insignificant.

Physically, the decrease of the scattering cross section, σ_{ps}, may be thought of as due to the changing relative phase of motion of the two parts of the pair of scatterers as the frequency of oscillation changes. As fare as the dipole resonance is concerned, the pair is simple a double oscillator, constrained by the matrix material and coupled by multiple scattering.[1] In a coupled, linear oscillator the single particle resonance splits into two; at the lower resonance the two components tend to move in phase, at the higher resonance they tend to move out of phase with respect to each other. Depending on the orientation of the axis of the two particles with respect to the incoming wave, these resonances are excited more or less strongly.[1,9] Destructive interference and partial cancellation of the shear waves scattered by each of the two scatterers takes place in the resonance region, resulting in a net decrease of the total scattered shear wave amplitude. Below the resonances the two parts of the oscillator tend to move in phase with respect to the matrix material. Above the resonances they move out of phase with respect to the matrix material.

The average monopole and quadrupole oscillations of the two parts of the oscillator in the case of urethane in syntactic foam seem to occur independently; the scattering cross sections are largely uneffected by considering the two scatterers as a double oscillator, Figure 4, although in the case of the monopole our limited resolution does not allow a firm conclusion. Only the average relative phase of the center of mass motions of the two parts of the oscillator, their dipole motion, appears to become coupled in the above sense.

We know from other, unpublished studies of ours that the detailed structure of the dipole resonance region depends on the cutoff, X_0. The major effects, however, the broadening and the decrease of the maximum of the mode conversion cross section, are invariant with respect to X_0. As X_0 decreases, the interference minimum induced by the high frequency out of phase dipole resonance shows up clearly at high volume concentrations of Pb in epoxy, not only in the cross sections and the attenuation, but also in the wave speed.

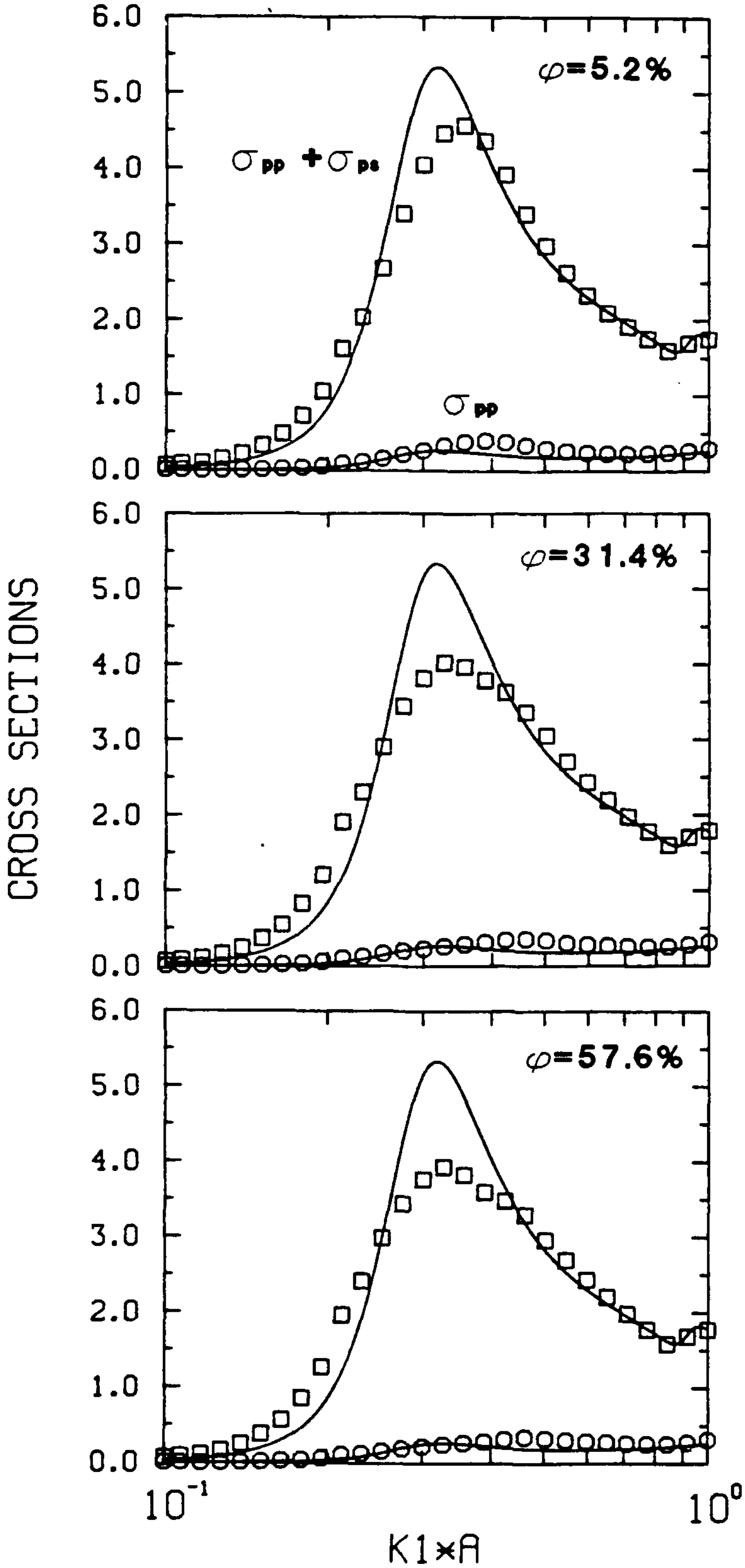

FIGURE 3. SCATTERING CROSS SECTIONS OF LEAD SPHERES IN EPOXY (EPON 828Z). (—) : SINGLE PARTICLES, (- O - , - □ -) : PAIRS OF PARTICLES AVERAGED OVER ORIENTATIONS AND CENTER-TO-CENTER SPACINGS

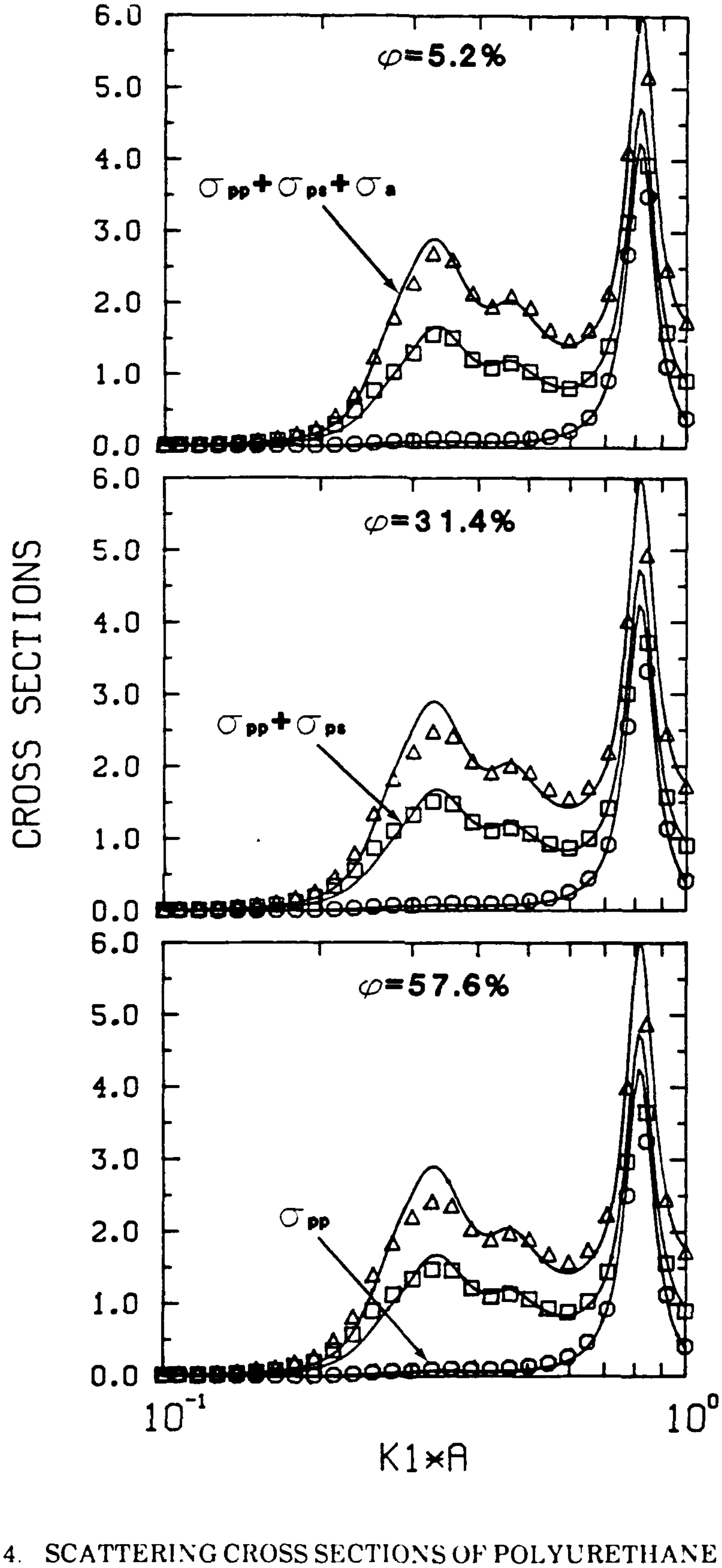

FIGURE 4. SCATTERING CROSS SECTIONS OF POLYURETHANE SPHERES IN SYNTACTIC FOAM. (—): SINGLE PARTICLES. (- O -, - □ -, - Δ -): PAIRS OF PARTICLES AVERAGED OVER ORIENTATIONS AND CENTER-TO-CENTER SPACINGS

WAVE SPEED

The most significant effects are observed in the case of Pb in epoxy, Figure 5. The dispersion region appears to broaden slightly in the pair scattering mode with increasing concentrations of inclusions and the single particle maximum between K1*A = .4 and .5 is greatly reduced. These effects appear to be due to the phase of relative motion as discussed above. In the case of urethane in syntactic foam on the other hand, multiple scattering, or coupling effects appear to be negligible at all concentrations of inclusions, Figure 6, again as expected from the discussion of the cross sections.

Some measurements of the wave speed for lead in epoxy resin are available.[10] They show that the dispersion minimum in the wave speed shifts to higher frequencies as the volume concentration of inclusions increases. The present results do not show this effect.

ATTENUATION

At low frequencies, attenuation due to pair scattering is enhanced by about a factor of two. Near the peak of the dipole resonance it is decreased somewhat, Figures 7 and 8, as expected from the discussion of the cross sections. The effects are most conspicuous for Pb in epoxy. Since attenuation and absorption are proportional to the appropriate cross sections, Figures 7, 8, and 9 would look exactly like the corresponding cross section plots if the ordinates were linear. Figure 3 therefore shows clearly that, e.g., at 57.6 percent Pb in epoxy peak attenuation in the pair scattering mode is reduced by about 25 percent. The difference between the two curves for pair scattering in Figure 8 is due to absorption, as explained above.

ABSORPTION

Comparing Figures 8 and 9 shows clearly that absorption in the viscoelastic polyurethane inclusions is a substantial part of the total attenuation mechanism in this material at all concentrations of inclusions; absorption and scattering make approximately equal contributions. Except at very low frequencies, either way of calculating absorption leads to essentially the same result, Figure 9. The irregular behavior of the points based on pair scattering in the low frequency region is not understood at present. It may be due to computational inaccuracies resulting from the finite shear loss tangent.

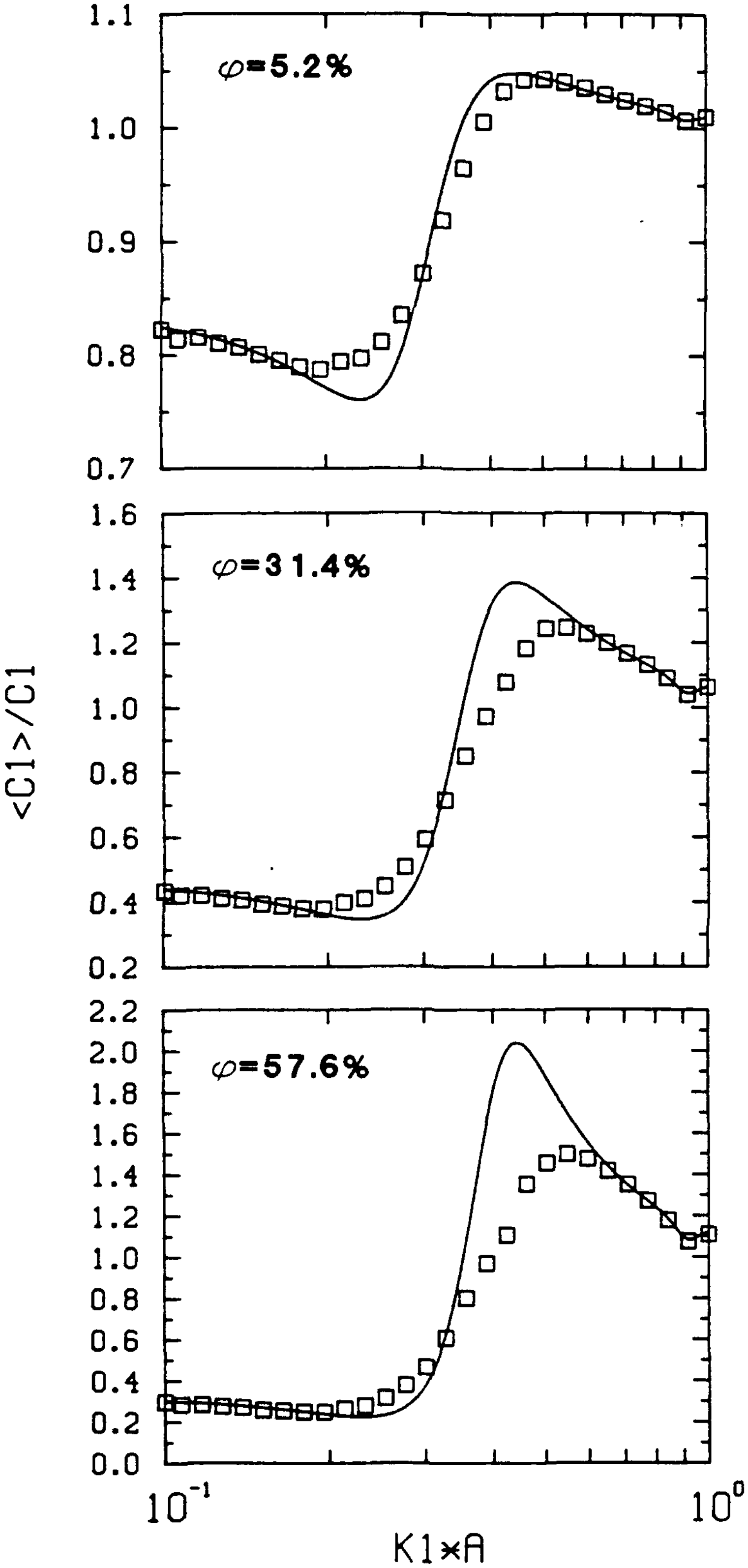

FIGURE 5. THE EFFECTIVE WAVE SPEED IN EPOXY (EPON 828Z) CONTAINING LEAD SPHERES, CALCULATED ON THE BASIS OF SINGLE PARTICLE SCATTERING (—) AND PAIR SCATTERING AVERAGED OVER ORIENTATIONS AND CENTER-TO-CENTER SPACINGS (- □ -)

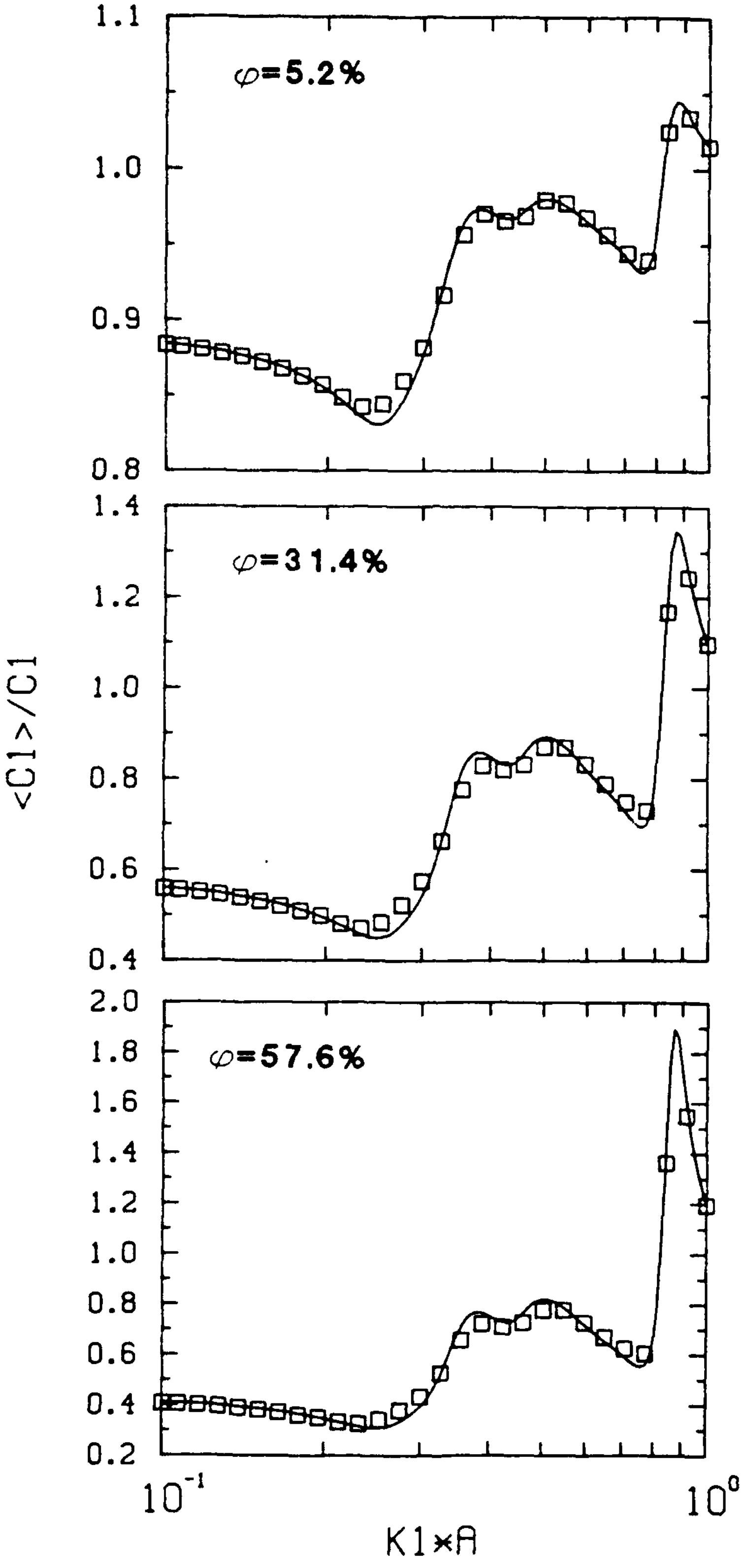

FIGURE 6. THE EFFECTIVE WAVE SPEED IN SYNTACTIC FOAM CONTAINING POLYURETHANE SPHERES, CALCULATED ON THE BASIS OF SINGLE PARTICLE SCATTERING (—) AND PAIR SCATTERING AVERAGED OVER ORIENTATIONS AND CENTER-TO-CENTER SPACINGS (-□-)

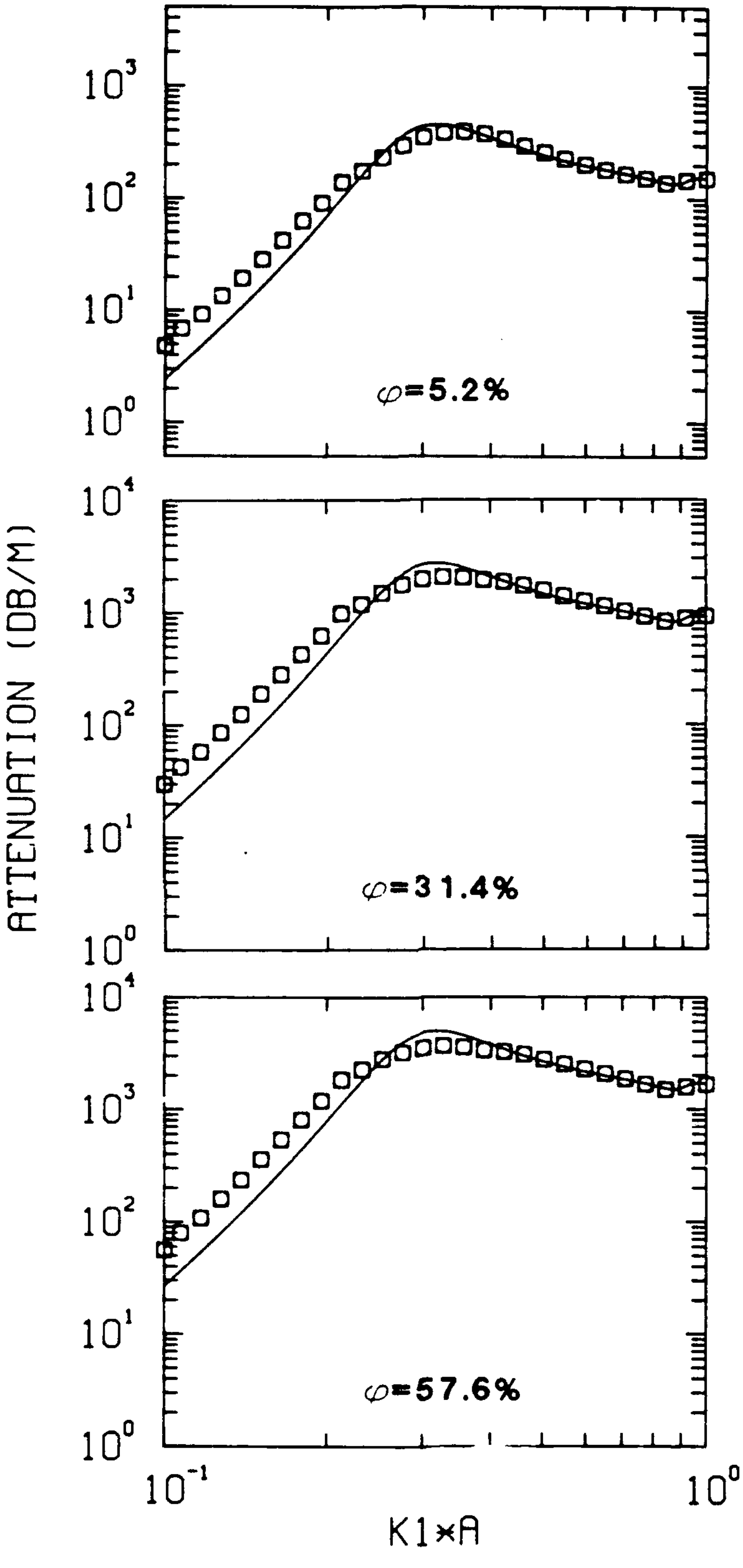

FIGURE 7. THE EFFECTIVE ATTENUATION IN EPOXY (EPON 828Z) CONTAINING LEAD SPHERES, CALCULATED ON THE BASIS OF SINGLE PARTICLE SCATTERING (—) AND PAIR SCATTERING AVERAGED OVER ORIENTATIONS AND CENTER-TO-CENTER SPACINGS (-□-). (-O-): ATTENUATION FOR AVERAGED PAIR SCATTERING PREDICTED BY $\sigma_{pp} + \sigma_{ps}$

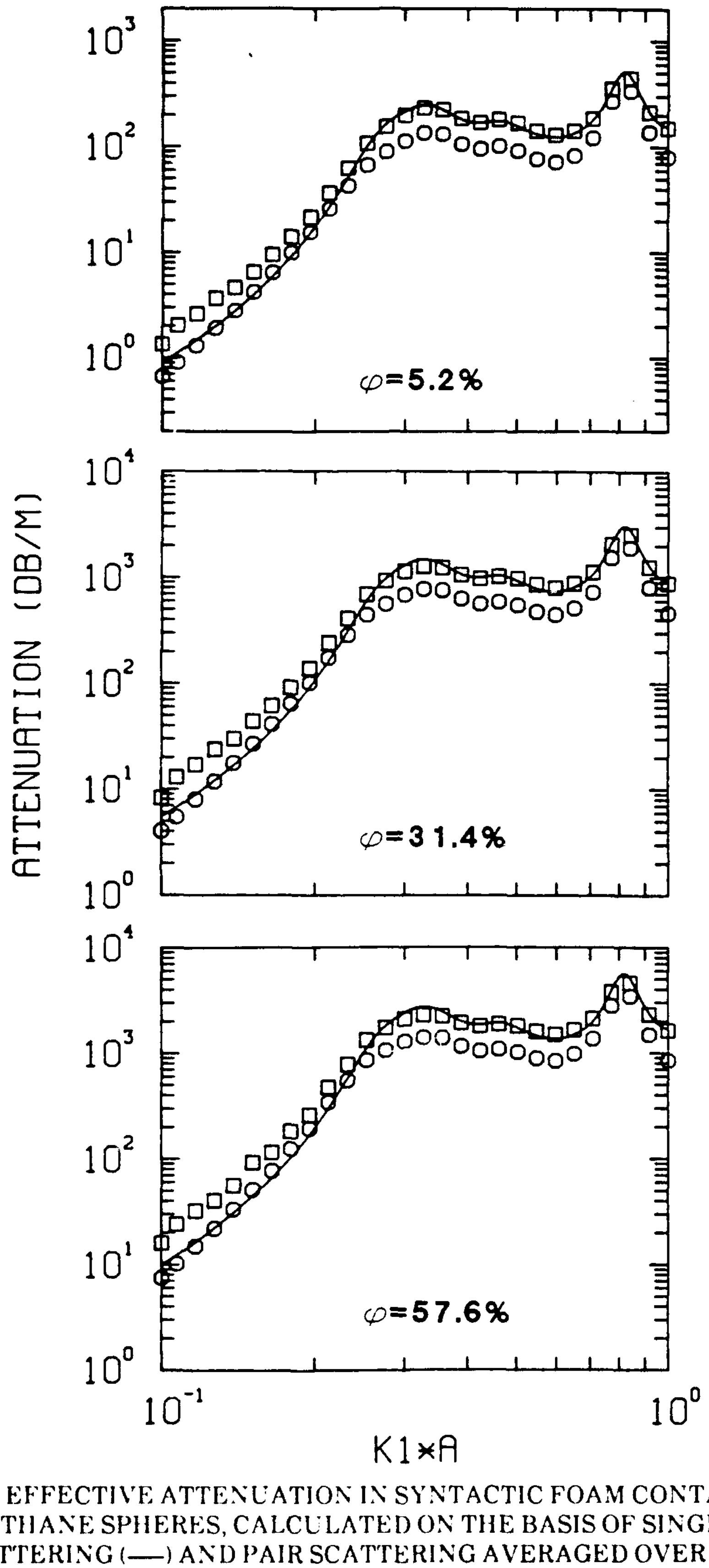

FIGURE 8. THE EFFECTIVE ATTENUATION IN SYNTACTIC FOAM CONTAINING POLYURETHANE SPHERES, CALCULATED ON THE BASIS OF SINGLE PARTICLE SCATTERING (—) AND PAIR SCATTERING AVERAGED OVER ORIENTATIONS AND CENTER-TO-CENTER SPACINGS (-□-). (-O-): ATTENUATION WITHOUT ABSORPTION FOR AVERAGED PAIR SCATTERING

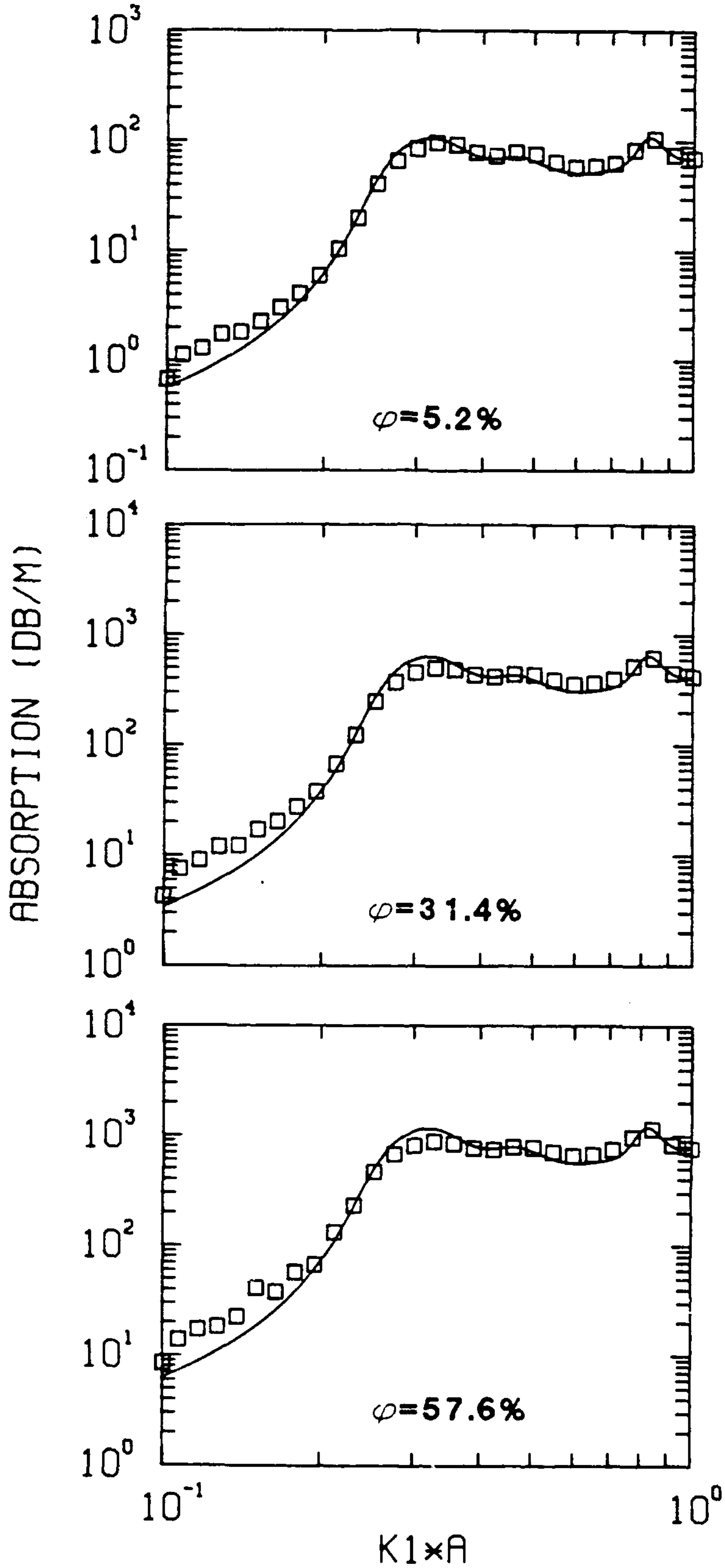

FIGURE 9. THE EFFECTIVE ABSORPTION IN SYNTACTIC FOAM CONTAINING POLYURETHANE SPHERES, CALCULATED ON THE BASIS OF SINGLE PARTICLE SCATTERING (—) AND PAIR SCATTERING AVERAGED OVER ORIENTATIONS AND CENTER-TO-CENTER SPACINGS (-□-)

CONCLUSIONS

Whereas some of the amplitude changes predicted by using pair scattering in place of single particle scattering in the case of Pb in epoxy are large enough to be measurable, in the case of the polyurethane-syntactic foam system the effects are probably in the noise, except perhaps for the level of low frequency attenuation. Moreover, no significant shifts in the frequencies of wave speed dispersion and the attenuation edge are predicted, except in the case of Pb in epoxy where the attenuation edge moves to somewhat lower frequencies.

The general absence of significant frequency shifts in the observable quantities points toward the fact that the splitting of the dipole resonance frequency due to coupling between the two oscillators of the pair of scatterers is weak. In the case of Pb in epoxy, however, this splitting appears to contribute toward moving the attenuation edge to somewhat lower frequencies. Destructive interference effects due to the high frequency resonance of the double oscillator lead to generally decreased amplitudes of observable quantities in the resonance region. Both frequency splitting and destructive interference are responsible for the broadening of the dipole resonance region, particularly in the case of Pb in epoxy.

REFERENCES

1. Scharnhorst, K. P.; Hackman, R. H.; and Lim, R., "An Application of the Forward Scattering Theorem to Elastic Wave Attenuation in Inhomogeneous Materials," 117th meeting of the Acoustical Society of America, Syracuse, NY, May 1989 and Scharnhorst, K. P., "On Wave Propagation in Inhomogeneous Media," Ultrasonics International 1989 Conference in Madrid, Spain, Jul 1989. The latter focusses on mixtures of solid inclusions and air bubbles.

2. Ishimaru, A., Wave Propagation and Scattering in Random Media, Vol. 2, Academic Press, NY, 1978.

3. Throop, G. J. and Bearman, R. J., "Numerical Solution of the Perkus-Yevick Equation for the Hard-Sphere Potential," The Journal of Chemical Physics, 42, 1965, p. 2408.

4. Varatharajulu, V. and Yih-Hsing Pao, "Scattering Matrix for Elastic Waves. I. Theory," J. Acoustical Soc. of America, 60, 1976, p. 556.

5. Yih-Hsing Pao, "Betti's Identity and Transition Matrix for Elastic Waves," J. Acoustical Soc. of America, 64, 1978, p. 302.

6. Gubernatis, J. E.; Domany, E.; and Krumhansl, J. A., "Formal Aspects of the Theory of Scattering of Ultrasound by Flaws in Elastic Materials," J. Appl. Phys., 48, 1977, p. 2804 and Gubernatis, J. E.; Domany, E.; Krumhansl, J. A.; and Huberman, M., "The Born Approximation in the Theory of Scattering of Elastic Waves by Flaws," J. Apply. Phys., 48, 1977, p. 2812.

7. Lim, R. and Hackman, R. H., "Comments on the Calculation of Cross Sections for Elastic Wave Scattering Using the T-Matrix," J. Acoustical Soc. of America, 87, 1990, p. 1070.

8. Bostroem, A., "Multiple Scattering of Elastic Waves by Bounded Obstacles," J. Acoustical Soc. of America, 67, 1979, 399.

9. Lim, R. and Hackman, R. H., "A Parametric Analysis of Attenuation Mechanisms in Composites Designed for Echo Reduction," J. Acoustical Soc. of America, 87, 1990, p. 1076.

10. Kinra, V. K. and Rousseau, C. Q., "Acoustical and Optical Branches of Wave Propagation, Some Additional Results," Symposium on Multiple Scattering of Waves in Random Media and Random Rough Surfaces, V. K. Varadan and V. V. Varadan, Editors, 1985.

11. Lim, R. and Hackman R., NCSC, private communication.

APPENDIX

AN ALGORITHM FOR THE T-MATRIX OF A PAIR OF SPHERICAL SCATTERERS OF ELASTIC WAVES

The T-matrix to be calculated is:[A-1]

$$T_p = R^t(d)T(1)\left(1-\sigma(2d)T(2)\sigma^t(2d)T(1)\right)^{-1}\left(R(d)+\sigma(2d)T(2)R^t(d)\right) +$$
$$R(d)T(2)\left(1-\sigma^t(2d)T(1)\sigma(2d)T(2)\right)^{-1}\left(R^t(d)+\sigma^t(2d)T(1)R(d)\right) \qquad \text{(A-1)}$$

where 2d is the distance between the scatterers, T is the single particle T-matrix and R and σ are translation operators.

We have analyzed this matrix in some detail and have used the insights gained to maximize the computational efficiency of our algorithm.

Of special interest is the case T(1) = T(2) for spherical scatterers with relative translations along the z-axis. In that case, we show that Equation (A-1) takes the form

$$T_p = A + PAP \qquad \text{(A-2)}$$

where A is the first term in Equation (A-1) and PAP the second (or vice versa). P is given below. Since P is a very simple matrix, essentially only one-half of T_p needs to be calculated and only one inversion needs to be performed.

The analysis was carried out in the space in which the polarization and parity indices are not mixed. Our algorithm also runs primarily in this space. We call this Space I. For computational efficiency, inversions must, however, be carried out in the space in which these indices are mixed.[A-2] We call the latter space Space II. The two spaces are related by a similarity transformation.

Using Pao's wave function convention,[A-3] the R and σ matrices for translations along the z-axis have the following form:

$$\begin{matrix} x_{11} & 0 & 0 & 0 & 0 & 0 \\ 0 & x_{22} & 0 & 0 & 0 & 0 \\ 0 & 0 & x_{33} & 0 & 0 & x_{36} \\ 0 & 0 & 0 & x_{44} & x_{45} & 0 \\ 0 & 0 & 0 & x_{54} & x_{55} & 0 \\ 0 & 0 & x_{63} & 0 & 0 & x_{66} \end{matrix} \qquad \text{(A-3)}$$

where each x_{ij} represents an "m-diagonal" system of square matrices, the one in the upper left hand corner being the largest (of dimension l_{max+1}, where l_{max} is the maximum mode index) corresponding to the azimuthal index $m = 0$, and the one in the lower right hand corner being a scalar (corresponding to the azimuthal index l_{max}):

$$x_{ij} \equiv \begin{bmatrix} \begin{pmatrix} \text{Dim.} \\ l_{max+1} \end{pmatrix} & & \\ & \begin{pmatrix} \text{Dim.} \\ l_{max} \end{pmatrix} \equiv x_{ij}(m) & 0 \\ 0 & \ddots & \\ & & \begin{pmatrix} \text{Dim.} \\ 1 \end{pmatrix} \end{bmatrix} \tag{A-4}$$

Every block of x, x(m), has the form

$$x(m) = \begin{matrix} s_{11} & a_{12} & s_{13} & a_{14} & \cdots \\ a_{21} & s_{22} & a_{23} & s_{24} & \cdots \\ s_{31} & a_{32} & s_{33} & a_{34} & \cdots \\ a_{41} & s_{42} & a_{43} & s_{44} & \cdots \\ \vdots & \vdots & \vdots & \vdots & \end{matrix} \tag{A-5}$$

where s_{ij} and a_{ij} are complex or real numbers (for σ and R, respectively) and they have the property that in the transpose of x(m), $x^t(m)$, a_{ij} has changed sign but s_{ij} has not:

$$x^t(m) = \begin{matrix} s_{11} & a_{12} & s_{13} & a_{14} & \cdots \\ a_{21} & s_{22} & a_{23} & s_{24} & \cdots \\ s_{31} & a_{32} & s_{33} & a_{34} & \cdots \\ a_{41} & s_{42} & a_{43} & s_{44} & \cdots \\ \vdots & \vdots & \vdots & \vdots & \end{matrix} \tag{A-6}$$

where $a_{ij} = -a_{ji}$ and $s_{ij} = s_{ji}$.

Hence, for any x_{ij} in Equation (A-3)

$$x^t_{ij} = D^{-1} x_{ij} D \tag{A-7}$$

where D has the form

$$D = \begin{pmatrix} \begin{pmatrix} +1 & & \\ & -1 & \\ & & \ddots \end{pmatrix} & & 0 \\ & \begin{pmatrix} +1 & & \\ & -1 & \\ & & \ddots \end{pmatrix} & \\ 0 & & \ddots \end{pmatrix} \quad \text{(A-8)}$$

and $D^2 = I$ or $D^{-1} = D$. This matrix may be thought of as a string of diagonal "m-blocks" along the main diagonal with alternating plus and minus ones, each block corresponding to some $\mathbf{x}(m)$ and starting with $+1$ in the upper left hand corner.

The structures of RT, σT, $R^t T$, $\sigma^t T$, $\sigma T(2)\sigma^t T(1)$, $\sigma^t T(1)\sigma T(2)$, etc., in fact the structures of all of the matrices in the various products in Equation (A-1), including that of T_p itself, are all the same and are of the form:

$$X = \begin{bmatrix} x_{11} & 0 & 0 & x_{14} & x_{15} & 0 \\ 0 & x_{22} & x_{23} & 0 & 0 & x_{26} \\ 0 & x_{32} & x_{33} & 0 & 0 & x_{36} \\ x_{41} & 0 & 0 & x_{44} & x_{45} & 0 \\ x_{51} & 0 & 0 & x_{54} & x_{55} & 0 \\ 0 & x_{62} & x_{63} & 0 & 0 & x_{66} \end{bmatrix} \quad \text{(A-9)}$$

where every x_{ij}-matrix has the form of Equation (A-4) and where in σT and RT, $x_{23} = x_{14} = 0$. Similarly for $\sigma^t T$ and $R^t T$. Focussing on $\sigma T(2)\sigma^t T(1)$, one finds that a typical x_{ij} has the form:

$$x = \sum_{k=1}^{N} \sigma(i_k)\, T(2,j_k)\, \sigma^t(l_k)\, T(l,n_k) \quad \text{(A-10)}$$

where $1 \le N \le 3$ and, e.g., $\sigma(i_k)$ is an element of the set

$$\left(\sigma_{11}^{ee}, \sigma_{11}^{oo}, \sigma_{22}^{ee}, \sigma_{22}^{oo}, \sigma_{23}^{eo} \right) \quad \text{(A-11)}$$

and

$$\sigma_{11}^{ee} \equiv x_{11}, \sigma_{11}^{oo} \equiv x_{22}, \sigma_{22}^{ee} \equiv x_{33} = x_{55}, \sigma_{22}^{oo} \equiv x_{44} = x_{66}, \sigma_{23}^{eo} \equiv x_{36} = -x_{45} = x_{54} = -x_{63}$$

in Equation (A-3) and all of these have the form of Equation (A-4). Also T_k is an element of the set

$$(T_{11}, T_{22}, T_{33}, T_{13}, T_{31}) \quad \text{(A-12)}$$

and it should be noted that T has the form:

$$T \equiv \begin{bmatrix} x_{11} & 0 & 0 & 0 & x_{15} & 0 \\ 0 & x_{22} & 0 & 0 & 0 & x_{26} \\ 0 & 0 & x_{33} & 0 & 0 & 0 \\ 0 & 0 & 0 & x_{44} & 0 & 0 \\ x_{51} & 0 & 0 & 0 & x_{55} & 0 \\ 0 & x_{62} & 0 & 0 & 0 & x_{66} \end{bmatrix} \qquad \text{(A-13)}$$

where $T_{11} = x_{11} = x_{22}$, $T_{22} = x_{33} = x_{44}$, $T_{33} = x_{55} = x_{66}$, $T_{13} = x_{15} = x_{26}$, $T_{31} = x_{51} = x_{62}$ in Equation (A-13) and all of the T_{ij} are diagonal (for spheres). In the case of elastic scatterers, $T_{ij} = T_{ji}^t$, i.e., $T_{13} = T_{31}$ for elastic spheres.

For $\sigma^t T(1)\sigma T(2)$ we have matrices of the form:

$$x = \pm \sum_{k=1}^{N} \sigma^t(i_k)\, T(1,j_k)\, \sigma(l_k)\, T(2,n_k) \qquad \text{(A-14)}$$

The sign in Equation (A-14) is positive if there are an even number of σ_{23}^{eo} in every term and negative otherwise. It can be shown that if $\sigma T(2)\sigma^t T(1)$ has the form shown in Equation (A-9), then $\sigma^t T(1)\sigma T(2)$ has the form:

$$X \equiv \begin{bmatrix} \bar{x}_{11} & 0 & 0 & -\bar{x}_{14} & \bar{x}_{15} & 0 \\ 0 & \bar{x}_{22} & -\bar{x}_{23} & 0 & 0 & \bar{x}_{26} \\ 0 & -\bar{x}_{32} & \bar{x}_{33} & 0 & 0 & -\bar{x}_{36} \\ -\bar{x}_{41} & 0 & & \bar{x}_{44} & -\bar{x}_{45} & 0 \\ \bar{x}_{51} & 0 & 0 & -\bar{x}_{54} & \bar{x}_{55} & 0 \\ 0 & \bar{x}_{62} & -\bar{x}_{63} & 0 & 0 & \bar{x}_{66} \end{bmatrix} \qquad \text{(A-15)}$$

where the sings are those in Equation (A-14). The exact relationship between a typical x_{ij} in Equation (A-9) and a typical $\bar{x}_{ij}$ in Equation (A-15) may now be found as follows. Using Equation (A-7):

$$\sigma(i_k)T(2,j_k)\sigma^t(l_k)T(1,n_k) = DD\sigma(i_k)DDT(2,j_k)D\sigma(l_k)DT(1,n_k)DD =$$

$$D\sigma^t(i_k)T(2,j_k)\sigma(l_k)T(1,n_k)D \qquad \text{(A-16)}$$

since the T-matrices are diagonal (for spheres).

Hence,

$$x_{ij} = \pm D\bar{x}_{ij}D \quad \text{and} \quad \bar{x}_{ij} = \pm D x_{ij} D \qquad \text{(A-17)}$$

if T(1) = T(2). Therefore, if T(1) = T(2), by assembling the D matrices into a "supermatrix," P, which also handles the sign changes on going from Equation (A-9) to Equation (A-15), we find that:

$$P = \begin{pmatrix} D & & & & & 0 \\ & -D & & & & \\ & & D & & & \\ & & & -D & & \\ & & & & D & \\ 0 & & & & & -D \end{pmatrix} = P^{-1} \qquad \text{(A-18)}$$

and

$$(1 - \sigma^{t}T\sigma T) = P(1 - \sigma T\sigma^{t}T)P \qquad \text{(A-19)}$$

Similarly,

$$(1 - \sigma^{t}T\sigma T)^{-1} = P(1 - \sigma T\sigma^{t}T)^{-1}P \qquad \text{(A-20)}$$

i.e., $(1-\sigma T\sigma^{t}T)^{-1}$ transforms exactly like $(1-\sigma T\sigma^{t}T)$. Similar considerations show (by inserting P^2 between the matrices) that P transforms any part of the first term of Equation (A-1), i.e., any pat of A, including A itself, into the corresponding part of the second term and vice versa. Hence, in analogy with Equation (A-20), the second part of T_p is:

$$B = PAP \qquad \text{(A-21)}$$

and

$$T_p = A + B \qquad \text{(A-22)}$$

if T(1) = T(2). This result depends only on the spherical geometry of the scatterers [Equation (A-16)], not on their elastic properties. The spheres may be elastic or viscoelastic.

SYMMETRIES AND COMPUTATIONAL SAVINGS

Upon studying the forms of $\sigma T(2)\sigma^{t}T(1)$ and $\sigma^{t}T(1)\sigma T(2)$ more closely, one finds with respect to the matrix elements in Equation (A-9), for $m < l_{max+1}$

$$\begin{aligned} x_{22} &= x_{11}\,,\ x_{32} = -x_{41}\,,\ x_{62} = x_{51} \\ x_{14} &= -x_{23}\,,\ x_{44} = x_{33}\,,\ x_{54} = -x_{63} \\ x_{26} &= x_{15}\,,\ x_{36} = -x_{45}\,,\ x_{66} = x_{55} \end{aligned} \qquad \text{(A-23)}$$

and similarly for x_{ij} in Equation (A-17) and, in fact, for all of the matrices and matrix products in Equation (A-1), including T_p itself. When $m = l_{max+1}$ one finds

$$x_{22} = x_{32} = x_{62} = x_{14} = x_{44} = x_{54} = x_{26} = x_{36} = x_{66} =$$

$$x_{41} = x_{63} = x_{23} = x_{45} \equiv 0. \qquad \text{(A-24)}$$

except for T(1) and T(2), where Equation (A-23) holds for all m.

If one transforms from Space I to Space II, where in every m-diagonal sub-block we count through all polarization and parity indices at fixed mode number, 1 (forming a 6*6 block for each 1) and repeat that count for all $1 \leq m$ (in every m-diagonal block), we find that the above symmetries hold between adjacent columns of the transformed matrix. This is the form of the matrix ($1-\sigma T \sigma' T$) that should be inverted because it is m-diagonal and may be inverted one block at a time, yielding much smaller matrices than in Space I. But because of the above symmetries between the elements it is not necessary to invert the whole matrix. Only every other column needs to be inverted; i.e., only 50 percent of every m-diagonal block in Space II needs to be inverted and, as shown above, only one inversion is necessary when $T(1) = T(2)$, reducing the computational effort by another 50 percent for a total reduction of computations associated with matrix inversion of 75 percent when $T(1) = T(2)$ and 50 percent when $T(1) \neq T(2)$.

Since the symmetries indicated in Equations (A-23) and (A-24) hold throughout all matrix manipulations, once RT, σT, $R'T$, and $\sigma' T$ have been formed it is only necessary to work with the nine blocks (1,1), (4,1), (5,1), (2,3), (3,3), (6,3), (1,5), (4,5), and (5,5) in Space I. The other nine non-zero blocks may be ignored. Since there are 36 blocks altogether, we thus only work with one quarter of the matrices, for a considerable savings in computational effort ($T(1) = T(2)$ or not). These nine blocks correspond to the odd numbered columns of ($1-\sigma T \sigma' T$) in Space II, which are the ones being inverted.

It should also be noted that in Space I the m-diagonal blocks, x(m), in Equation (A-4) are densely populated with non-zero elements, whereas in Space II all of the zero blocks in Equation (A-9) are carried and stored. It is therefore preferable to work in Space I when matrix multiplications are performed since many zero manipulations are avoided and only the indicated subset of nine matrix blocks is considered. This then is the space in which most of our calculations are being performed. On the other hand, for matrix inversions, Space II is indispensible.

THE STRUCTURE OF THE ALGORITHM

1. Do the matrix multiplications to arrive at ($1-\sigma T \sigma' T$) in Space I.

2. For the inversions of ($1-\sigma T \sigma' T$) do the similarity transformation which takes this matrix into Space II. This amounts to nothing more than a repacking of the matrix into m-diagonal blocks and requires no greater computational effort than loading it in the first place.

3. Invert very other column of this matrix. If $T(1) \neq T(2)$ do the same for ($1-\sigma' T \sigma T$).

4. Do the inverse similarity transformation to take $(1-\sigma T \sigma' T)^{-1}$ back into Space I. Again, this amounts to no more than an unpacking of the matrix into the nine working blocks of Space I. If $T(1) \neq T(2)$ do the same for $(1-\sigma' T \sigma T)^{-1}$.

5. Perform the remaining matrix manipulations in Space I. For T(1) = T(2), calculate either the first or the second part of Equation (A-1), then use Equation (A-21) to obtain T_p.

By properly sequencing the computations, storage space may be minimized. Also, in the case of elastic spherical scatterers, it is only necessary to calculate

$$R^t T(1)(1 - \sigma T(2)\sigma^t T(1))^{-1} \sigma T(2) R^t \tag{A-25}$$

or

$$R T(2)(1 - \sigma^t T(1)\sigma T(2))^{-1} \sigma^t T(1) R \tag{A-26}$$

since one is the transpose of the other.

The results may be checked by observing that:

1. T_p must be symmetric for elastic materials (true for any T-matrix when absorption is zero).

2. The T-matrix theorem must hold, i.e.,

$$-\text{Real}(T_p) = T_p T_p^* \tag{A-27}$$

3. In the special case of T(1) = T(2) we note from Equation (A-2) that

$$T_p = P T_p P \tag{A-28}$$

where T_p has the structure of Equation (A-9), is m-block diagonal in every x_{ij} and every x_{ij} has the form of Equation (A-5). Hence, since this transformation changes the sign of every other off-diagonal element in every m-block, Equation (A-28) implies that every other off-diagonal element in very m-block of T_p must be zero.

It should also be noted that the transformation from A to B in Equation (A-21) or from $(1\text{-}\sigma T \sigma^t T)$ to $(1\text{-}\sigma^t T \sigma T)$, etc., reduces to the nine, simple manipulations:

$$\bar{x}_{11} = D x_{11} D \,,\ \bar{x}_{41} = -D x_{41} D \,,\ \bar{x}_{51} = D x_{51} D$$

$$\bar{x}_{23} = -D x_{23} D \,,\ \bar{x}_{33} = D x_{33} D \,,\ \bar{x}_{63} = -D x_{63} D$$

$$\bar{x}_{15} = D x_{15} D \,,\ \bar{x}_{45} = -D x_{45} D \,,\ \bar{x}_{55} = D x_{55} D \,.$$

REFERENCES

A-1. Bostroem, A., "Multiple Scattering of Elastic Waves by Bounded Obstacles," J. Acoustical Soc. of America, 67, 1979, 399.

A-2. Lim, R. and Hackman R., NCSC, private communication.

A-3. Yih-Hsing Pao, "Betti's Identity and Transition Matrix for Elastic Waves," J. Acoustical Soc. of America, 64, 1978, p. 302.

DISTRIBUTION

	Copies
Office of the Chief	
of Naval Research	
Attn: ONR Code 1131F	
(Wallace Smith)	1
ONR Code 1132SM	
(Albert Tucker)	1
(Stephen Newfield)	1
ONR Code 1223 (Geoff Main)	1
ONT Code 233	
(Gene Remmers)	1
ONT Code 234	
(Thomas Warfield)	1
ONT Code 235	
(Wally Ching)	1
800 N. Quincy Street	
Arlington, VA 22217-5000	
Commander	
Naval Sea Systems Command	
Attn: Code 55W (J. Keggler)	1
Washington, DC 20362	
Commander	
Naval Research Laboratory	
Attn: Code 5135 (R. Corsaro)	1
Washington, DC 20375	
Commander	
Naval Underwater Systems Center	
Attn: R. Radlinksi	1
Library	1
New London Laboratory	
New London, CT 06320	
Commander	
Naval Torpedo Station	
Attn: C. Thurman	1
Library	1
Keyport, WA 98345	

	Copies
Commander	
David Taylor Research Center	
Attn: F. Desiderati	1
S. McKeon	1
J. Dlubac	1
D. Zadra	1
Library	1
Bethesda, MD 20084	
Commander	
David Taylor Research Center	
Attn: Code 2842 (A. Santiago)	1
Technical Library	1
Annapolis Laboratory	
Annapolis, MD 21402	
Commander	
Naval Ocean Systems Center	
Attn: Library	1
San Diego, CA 92152	
Commander	
Naval Coastal Systems Center	
Attn: Technical Library	1
Panama City, VL 32407	
Commander	
Naval Technical Intelligence Center	
Attn: Library	1
4301 Suitland Road	
Washington, DC 20023	
Commanding Officer	
More Island Naval Shipyard	
Attn: B. Jan	5
Ship Silencing Branch	
Vallejo, CA 94592	

DISTRIBUTION (Cont.)

	Copies
Commanding Officer Underwater Sound Reference Division Attn: Dr. C. Thompson	1
Dr. R. Ting	1
Dr. R. N. Capps	1
Technical Library	1
Orlando, FL 32806	
General Dynamics/Eastern Point Road Electric Boat Division Attn: J. Krause	1
Groton, CT 06340	
Pennsylvania State University Applied Research Laboratory Attn: S. Hayek	1
Library	1
P.O. Box 30 State College, PA 16804	

	Copies
Defense Technical Information Center Cameron Station Alexandria, VA 22304-6145	1
Internal Distribution:	
E231	3
E232	2
E35	1
U	1
U077 (T. M. Ryczek)	1
R	1
R30	2
R31	1
R31 (W. Madigosky)	1
R31 (K. Scharnhorst)	10

REPORT DOCUMENTATION PAGE

Form Approved OMB No. 0704-0188

1. AGENCY USE ONLY *(Leave blank)*

2. REPORT DATE
20 March 1991

3. REPORT TYPE AND DATES COVERED
Interim

4. TITLE AND SUBTITLE
Effective Dynamic Material Parameters and Localized Scattering

5. FUNDING NUMBERS
PE61152N
PRZR00001
TAZR01108
WUR01AA860

6. AUTHOR(S)
Kurt P. Scharnhorst

7. PERFORMING ORGANIZATION NAME(S) AND ADDRESS(ES)
Naval Surface Warfare Center
10901 New Hampshire Avenue
Silver Spring, Maryland 20903-5000

8. PERFORMING ORGANIZATION REPORT NUMBER
NAVSWC TR 91-182

9. SPONSORING/MONITORING AGENCY NAME(S) AND ADDRESS(ES)
Naval Surface Warfare Center
10901 New Hampshire Avenue
Silver Spring, Maryland 20903-5000

10. SPONSORING/MONITORING AGENCY REPORT NUMBER

11. SUPPLEMENTARY NOTES

12a. DISTRIBUTION/AVAILABILITY STATEMENT
Approved for public release; distribution is unlimited.

12b. DISTRIBUTION CODE

13. ABSTRACT *(Maximum 200 words)*

A modification of the classical effective wave vector in randomly inhomogeneous media

$$k_p^* = k_p + 2\pi n f_p(1,0)/k_p$$

is discussed, which replaces the single particle far field forward scattering amplitude, $f_p(1,0)$, by an average pair scattering amplitude, $\bar{f}_p(2,0)$. The Perkus-Yevick radial distribution function is used to find the average of $f_p(2,0)$ over radial separations extending to the first nearest neighbor maximum. The results is applied to random distributions of mass loaded polyurethane spheres in syntactic foam and to lead spheres in an epoxy resin matrix and compared with calculations based on the single particle amplitude. We find that in the case of high concentrations of lead inclusions in epoxy, the mode conversion cross section as well as the real and imaginary parts of the effective wave vector are significantly altered by pair scattering. In the case of mass loaded polyurethane in syntactic foam, on the other hand, the effects are negligible.

14. SUBJECT TERMS
Effective Dynamic Material Parameters, Acoustic Scattering, Pair Scattering, Mode Conversion

15. NUMBER OF PAGES
42

16. PRICE CODE

17. SECURITY CLASSIFICATION OF REPORT	18. SECURITY CLASSIFICATION OF THIS PAGE	19. SECURITY CLASSIFICATION OF ABSTRACT	20. LIMITATION OF ABSTRACT
UNCLASSIFIED	UNCLASSIFIED	UNCLASSIFIED	SAR

GENERAL INSTRUCTIONS FOR COMPLETING SF 298

The Report Documentation Page (RDP) is used in announcing and cataloging reports. It is important that this information be consistent with the rest of the report, particularly the cover and its title page. Instructions for filling in each block of the form follow. It is important to ***stay within the lines*** to meet ***optical scanning requirements***.

Block 1. Agency Use Only *(Leave blank)*.

Block 2. Report Date. Full publication date including day, month, and year, if available (e.g. 1 Jan 88). Must cite at least the year.

Block 3. Type of Report and Dates Covered. State whether report is interim, final, etc. If applicable, enter inclusive report dates (e.g. 10 Jun 87 - 30 Jun 88).

Block 4. Title and Subtitle. A title is taken from the part of the report that provides the most meaningful and complete information. When a report is prepared in more than one volume, repeat the primary title, add volume number, and include subtitle for the specific volume. On classified documents enter the title classification in parentheses.

Block 5. Funding Numbers. To include contract and grant numbers; may include program element number(s), project number(s), task number(s), and work unit number(s). Use the following labels:

C	- Contract	**PR**	- Project
G	- Grant	**TA**	- Task
PE	- Program Element	**WU**	- Work Unit Accession No.

BLOCK 6. Author(s). Name(s) of person(s) responsible for writing the report, performing the research, or credited with the content of the report. If editor or compiler, this should follow the name(s).

Block 7. Performing Organization Name(s) and Address(es). Self-explanatory.

Block 8. Performing Organization Report Number. Enter the unique alphanumeric report number(s) assigned by the organization performing the report.

Block 9. Sponsoring/Monitoring Agency Name(s) and Address(es). Self-explanatory.

Block 10. Sponsoring/Monitoring Agency Report Number. *(If known)*

Block 11. Supplementary Notes. Enter information not included elsewhere such as: Prepared in cooperation with...; Trans. of...; To be published in.... When a report is revised, include a statement whether the new report supersedes or supplements the older report.

Block 12a. Distribution/Availability Statement. Denotes public availability or limitations. Cite any availability to the public. Enter additional limitations or special markings in all capitals (e.g. NOFORN, REL, ITAR).

- **DOD** - See DoDD 5230.24, "Distribution Statements on Technical Documents."
- **DOE** - See authorities.
- **NASA** - See Handbook NHB 2200.2
- **NTIS** - Leave blank.

Block 12b. Distribution Code.

- **DOD** - Leave blank.
- **DOE** - Enter DOE distribution categories from the Standard Distribution for Unclassified Scientific and Technical Reports.
- **NASA** - Leave blank.
- **NTIS** - Leave blank.

Block 13. Abstract. Include a brief ***(Maximum 200 words)*** factual summary of the most significant information contained in the report.

Block 14. Subject Terms. Keywords or phrases identifying major subjects in the report.

Block 15. Number of Pages. Enter the total number of pages.

Block 16. Price Code. Enter appropriate price code ***(NTIS only)***

Blocks 17.-19. Security Classifications. Self-explanatory. Enter U.S. Security Classification in accordance with U.S. Security Regulations (i.e., UNCLASSIFIED). If form contains classified information, stamp classification on the top and bottom of the page.

Block 20. Limitation of Abstract. This block must be completed to assign a limitation to the abstract. Enter either UL (unlimited) or SAR (same as report). An entry in this block is necessary if the abstract is to be limited. If blank, the abstract is assumed to be unlimited.